The Design and Fabrication of a Micro Mechanical Dragonfly

Project Report
Submitted March 19, 2009

Patrick J. Lingane
Senior Thesis
William D. Keat, Advisor

Department of Mechanical Engineering
Union College
Schenectady, NY

Table of Contents

1. Abstract

The goal this project was to create a scaled model of a flapping wing aerial vehicle. The design was initially based on a remote controlled model available at many toy stores. This model was in the form of a dragonfly but about four times the size in each dimension. My project was to scale this down, ideally to the size of a real dragonfly. This however was difficult, and a half scaled prototype (twice life size) was constructed instead. Scaling was done using dimensionless fluid parameters such as the Reynolds and Strouhal numbers which effectively related the various properties of each model. Testing and modification of the prototype were carried out, and in the process an analytical model was made to model the dynamics. Although still not flying, the prototype will hopefully soon be ready for testing against the theory. In the future, more testing will be completed, and minor modifications made to get the scaled prototype flying. All of this is part of a larger goal to miniaturize a flapping flying robot of which this project is only a part.

2. Introduction

Flight has always fascinated humans, and it has only been during the past hundred years that humans have achieved powered flight. However the type of flight used in nature is different from what humans use; powered flight in nature uses flapping wings while human machines typically do not. There are advantages and disadvantages to each design although flapping wings are the only practical method of propulsion for animals. Typically humans have used rotating shafts or great amounts of heat to produce power, and neither of these things is available to animals.

With the recent advances in technology, more methods are available to create powered flight for man-made vehicles. Flapping flight provides certain challenges especially to our understanding of its motion, but also provides certain benefits that could not be realized without it. The fundamental difference between flapping and non-flapping flight is that flapping flight inherently uses non-steady state aerodynamic mechanisms to produce lift and thrust. Steady state aerodynamic technique, which has been successfully used in the past, is easier to analyze than non-steady state, and there has not been a reason to change. Recently however, people have realized the advantages of flapping flight, and technology has been created to analyze it.

Flapping flight is capable of producing much more maneuverability than fixed wing flight, and can also give sufficient lift to slower or even hovering vehicles. These advantages are offset by an increase in sensitivity to even the smallest of changes in motion, and control of these vehicles is much more difficult. Once these difficulties are overcome, these vehicles can be very useful. They may be used to carry cameras to survey a scene or find an injured person in a dangerous environment. They also give us a better sense of how nature operates, and could be interesting to entomologists.

There are various toys available that use flapping wings to power small craft either with or without remote control, and these can be bought cheaply. An example of this kind of toy is the WowWee Robotic Dragonfly available at Wal-Mart® stores and shown in Figure 1 or a similar robotic bat found at RadioShack®. My project sought to miniaturize the WowWee model to something more close to life sized. This was broken into various steps; the first was to create a proof of concept half-scale prototype using the same mechanisms as the original model. This was the primary goal of the project. Further goals

included finding a mechanism that can be scaled down past half scale, and finally building a prototype at that smaller scale. From the beginning however it was realized that in the time available for the project no smaller prototype would be designed or built, but only possibly a mechanism designed that is capable of motion at this small scale.

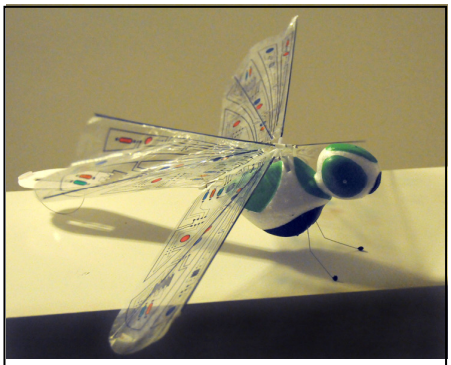

Figure 1: The WowWee Dragonfly

The original WowWee model had a wingspan of 0.41 meters. Large dragonflies have a wingspan of roughly a quarter of that. The mechanism used on this original WowWee model uses a geared rotary motor to turn a crankshaft, which connects to the wings through a connecting rod forming a four bar linkage for each set of two connected wings. The wings are arranged two on top and two on bottom, with each top wing connected rigidly to the opposite bottom wing so that the wings form an X when open.

This is an inexpensive way to provide wing motion, but has scaling limitations. The main goal of my project was to miniaturize the existing model and mechanism, and to arrange the new properties so that it will act and fly like the original. For any given size, a certain weight, flapping frequency and velocity are necessary to produce flight. My first goal was to define these variables. My second goal was to create a SolidWorks model that exhibited the correct motion and used parts that could readily be purchased. My third goal was to create a prototype that flew. When the first prototype did not fly, various modifications were made. As is par for the course, new problems arose in the process of which one in particular sparked the creation of an analytical model of the motion of the dragonfly using Matlab®. Results from this model as well as intuition and trial and error

led to the further improvement of the prototype which, near the end of the project, showed clear signs of forward movement while failing a flight test and crashing, still flapping, on the ground.

Goals of future work include continued modification to make the prototype fly, further testing and modification to update the analytical model, and finally design and fabrication of a smaller version of the prototype more comparable to the size of a real dragonfly.

3. Reverse engineering of the WowWee model

In order to effectively scale all the design parameters of the prototype, the original WowWee model was completely reverse engineered to find all its important design characteristics. Many experiments were performed during this process and are described here; Appendix A contains all the resulting data.

As a first experiment, the WowWee dragonfly was taken outside and flown around the yard. There were two controls for the dragonfly: throttle and turning. Each was controlled using a joystick on the remote control. The throttle stick controlled the frequency of flapping while the turning stick controlled the speed of a small propeller mounted sideways in the tail of the dragonfly. The model flew easily, though it was not easily controllable. Flight times ranged between five and thirty seconds before crashing, depending on wind conditions and the experience of the pilot. Some altitude gain was possible but proved difficult without stalling. A setting of beginner or expert controlled the sensitivity of the turning stick, and while in beginner mode the dragonfly turned little, in expert mode the turning became disruptive to the flight. One charge of the battery

produced about half an hour of fun, or about twelve to fifteen minutes of flight. The model thus flew well overall but still had some issues relating to control. However, for my project, control was a minor consideration and thus for my purposes the model flew successfully.

To analyze the wing motion, the model dragonfly was secured to a black surface and sufficient light was shown upon it. A Nikon model D300 camera was used in its rapid exposure mode to take pictures at seven frames per second of the dragonfly from both front and side. While taking these pictures, the dragonfly was run with a frequency very slightly faster than the camera speed such that in each picture the wings were in a slightly different position having just gone through slightly more than a full cycle. This produced a series of pictures which if viewed in order gave the appearance of smooth flapping flight which could be viewed frame by frame. In effect this was a cheap alternative to using a high speed camera for the same purpose. Eight of these images are arranged in Figure 2, and a more extensive set may be seen in Appendix A.

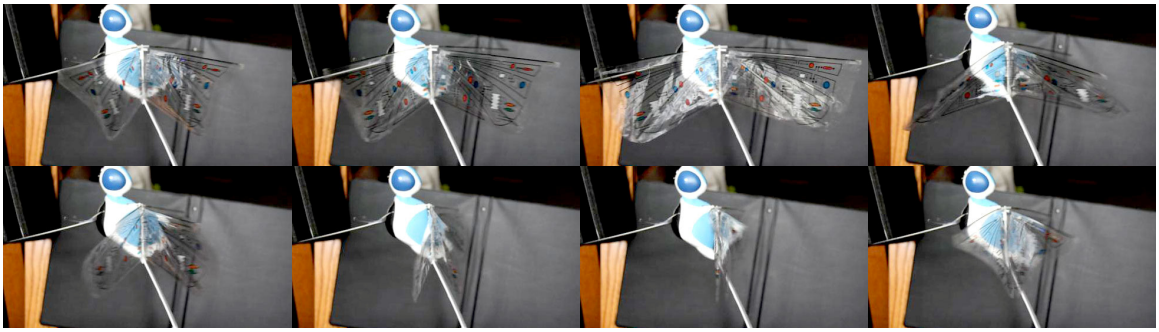

Figure 2: Motion series of the WowWee dragonfly

These pictures show that the thin, flat, flimsy airfoil of each of the WowWee dragonfly's wings deform during flight to become somewhat more of a traditional curved airfoil with the forward edge leading the trailing edge, and the curvature of the wing concave toward the direction of travel. This produces several advantages. If the wings did

not deform, no thrust would be generated by flapping. The wings operate much like the sail in a sailboat, changing the direction of the airflow impinging on them from vertical to backward. Although there is little wind actually traveling vertically, the flapping is a vertical motion which causes the relative wind on the wing to be vertical. When the wings come together, air is forced out behind the wings creating thrust. Putting a hand behind the flapping wings verifies that some thrust is generated by the wind that can be felt. Another advantage of the deformable wings is increased lift while gliding when the flat airfoil deforms into a more effective shape. This lift is particularly evident if the wings are not flapping, and only occurs during forward flight. Since the pictures in Appendix A do not represent forward flight, this effect is not observed there; only the flapping effect is present.

The pictures taken from the front (see Appendix A) do not provide as much information about the flight mechanism, but do provide some information on the rigidity of the wing rods which support the airfoils. These rods can be seen bending during flapping such that the phase at the tip of the wing is slightly behind the phase near the center. This is most likely undesirable, but since the magnitude of this bending is low, it likely has a negligible effect. From these pictures we can also see the changing shape of the airfoils as described previously.

The flapping frequency is an important parameter to measure for this mode of flight, and it was measured using a microphone. A microphone connected to a computer was mounted next to the model dragonfly such that at the extreme of every flap the wing rod hit the microphone. This produced a sharp sound with every hit while the motor sounds were steadier. Using the Sound Recorder application in Windows, the sound was

recorded for exactly ten seconds then slowed down to one eighth speed. The number of sharp taps could now be counted. Dividing the total number of taps by the original ten seconds provided an accurate measure of the flapping frequency at 9.45 Hz.

An experiment to determine the center of gravity of the model was completed for both the vertical and horizontal directions. First the model was hung by a thin ribbon attached to its tail to determine the vertical center of gravity. A picture was taken from the side of the model such that the ribbon was vertical in the frame. Any error here was corrected using the rotate features of Adobe Photoshop. A ruler was also mounted behind the model to give a size comparison. A second picture was taken of the model resting on two pointed objects to measure the horizontal center of gravity. These two objects were uncapped pens due to lack of a better apparatus, but they proved to work well. The model was balanced on these under the wings such that the tail was parallel to the horizontal floor. A second photograph was taken, and any camera rotation was corrected again using Photoshop. Vertical lines were drawn through the supports in each of these pictures to give a center of gravity in each. Finally these two images were superimposed and adjusted (scale, rotation, position) so that the dragonfly in each appeared in exactly the same place. The vertical lines drawn in each picture were now perpendicular, and crossed at the center of gravity. It is assumed that the center of gravity left to right is exactly at the center of the model. The resulting superimposed image may be seen in Figure 3.

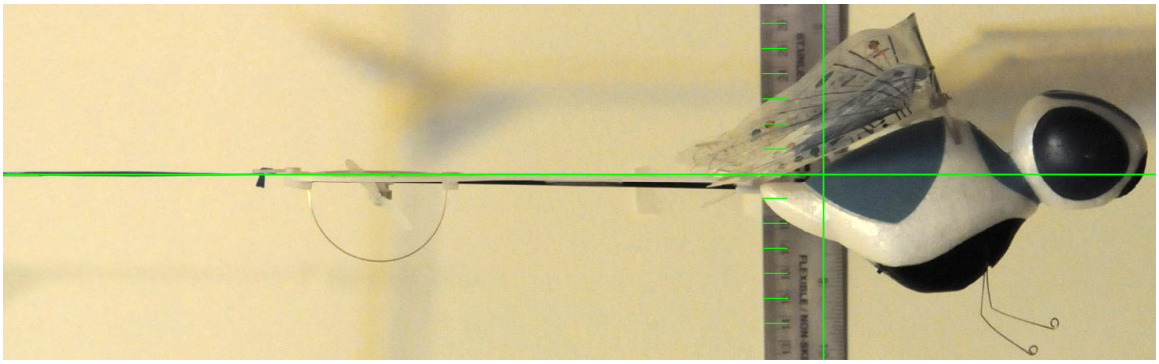

Figure 3: Determination of the center of gravity

The forward flight speed was determined by flying the model down a course of a known length, and letting it crash into a wall at the end. Since it was very difficult to control the model, a course of twenty feet was chosen at the end of a long hallway. At the end of the course, the hallway turned a corner presenting a wall straight ahead. During each flight, seconds were counted off verbally. This verbal timing was checked against a clock periodically to ensure accuracy, and provided resolution to one quarter of a second. More accuracy could have been attained using a stopwatch, but none was needed, for the flight speed varied significantly between trials. For an even flight with few stalls or dips, the 20 foot flight took just less than three seconds, so a speed was estimated using a time of 2.9 seconds. This speed was 2.1 meters per second after conversions. The slowest flight recorded had many stalls and dips, and had a speed of 1.6 meters per second. The steady state speed was taken to be the maximum flight speed because of the absence of dips and stalls during that trial.

Figure 4: The flapping mechanism

Finally, to analyze the kinematics of the motion and to measure weights and sizes of each component, the model was disassembled. The overall mass before disassembly was 23.7 grams. The other component masses, dimensions and specifications are listed in Appendix A. The battery had specifications printed on it. The kinematics (see Figure 4) were comprised of two four bar linkages sharing two links. The fixed link was the body, and a crankshaft was shared by both wings. The crank was a single component made of bent wire, but it contained two different axes on which each linkage operated. Its principal axis passed through the gears connected to the main motor, and it was then bent using an offset such that a second section was parallel to the main axis but offset slightly. A second offset bend created a third section also parallel to the main axis and offset the same amount as the second section, but at a different angle than the second section. Connecting rods were fitted loosely over the second and third sections and connected to the hinges at the top that held the wings. These hinges rotated about a fixed axis, and one

of the four wings was inserted into each side of each of the hinges. The connecting rods connected to a point a short distance away from the axis of the hinge so that when the crankshaft rotated the hinges also rotated. For a full revolution of the crankshaft, the hinges moved within about 42 degrees, creating a separation at the fully open position of 85 degrees and at the closed position of 0 degrees.

4. The dimensional scaling analysis

In order to most accurately scale the WowWee model down to a smaller size, the principles of dynamic similarity were used to find the characteristics of the smaller design. If two objects are dynamically similar, some key dimensionless parameters will be the same, and the fluid flow around them will be the same. In order to begin this process, the characteristics of the WowWee model were found experimentally as described in the previous section. Then the dimensionless quantities such as the Reynolds number and the Strouhal number were calculated from these characteristics. Since two models with equal dimensionless parameters will perform exactly equally, these parameters were applied to the scaled down version. A scaling factor was chosen, and from this and the original characteristics, new characteristics such as length, speed, and weight were calculated.

Arguably the most important and commonly used dimensionless parameter for fluid flows is the Reynolds number. The Reynolds number is a function of the dynamic viscosity (μ), density (ρ), characteristic velocity (V), and characteristic length (L). In this case the characteristic velocity was taken as the average forward velocity of the body of the dragonfly, while the characteristic length was the chord length (from the leading to

the trailing edge of the wing). The Reynolds number is calculated in Equation 1:

$$\mathrm{Re} = \frac{\rho V L}{\mu} = 11200 \tag{1}$$

In the case of a dragonfly, frequency is a very important factor because of the unsteady aerodynamics that give it lift and thrust. The only well known dimensionless parameter that incorporates frequency is the Strouhal number. It is calculated in Equation 2 from flapping frequency (*f*), velocity and characteristic length.

$$St = \frac{fL}{V} = 0.362 \tag{2}$$

One significant assumption in basic fluid mechanics is the incompressibility of air. When air is compressible, the aerodynamic flow changes dramatically. For most purposes, air may be considered to be incompressible if the speed of the aerodynamic object of interest is less than three tenths the speed of sound (c_{sound}). This is specified using the Mach number.

$$Ma = \frac{V}{c_{sound}} = 0.0268 < 0.3 \tag{3}$$

Compressible flow must be considered when the Mach number exceeds 0.3. From this Mach number it is clear that there is no compressibility. In a worst case scenario, where the Mach number changes with the inverse cube of the scaling factor, there is still no compressibility for a scaling factor of ½. Therefore future analysis disregarded the Mach number completely.

One important specification of the design of any flying object is its weight. The forces acting on the dragonfly must sum to zero if the object is in steady flight. For this to be possible, the lift force must equal the weight. Since the weights may not be the same

between the two scaled models, the lift coefficient was calculated which compares this and other quantities using a dimensionless parameter. A is the wing area, and F_L is the force of lift which is equal to the weight.

$$C_L = \frac{F_L}{\frac{1}{2}\rho V^2 A} = 5.24 \tag{4}$$

Lastly a scaling factor was introduced between the WowWee model and the new "scaled down" design. This scaling factor was meant to change the geometry of the wings in two dimensions where R is the length (radius) of the wing. This was chosen to be 0.5.

$$F_S = \frac{L_{scaled}}{L_{WowWee}} = \frac{R_{scaled}}{R_{WowWee}} = 0.5 \tag{5}$$

In order to achieve dynamic similarity, it was necessary to derive the quantities that were to change using the scaling factor and other dimensionless parameters. The following represents a list of the quantities that changed using this analysis and the equations which governed how they changed. These equations are simply equations 1 through 6 rewritten in various ways.

$$L_{C-scaled} = L_{C-WowWee} \cdot F_S \tag{5a}$$

$$R_{scaled} = R_{WowWee} \cdot F_S \tag{5b}$$

$$V = \frac{\mathrm{Re}\,\mu}{\rho L} \tag{1a}$$

$$f = \frac{StV}{L} \tag{2a}$$

$$F_L = C_L \cdot \tfrac{1}{2}\rho V^2 A \tag{4a}$$

This analysis produced values for certain parameters which were unattainable. These and other parameters are listed in Table 1 under the column "Scaled Design." For

example, the scaled design weighs as much as the larger model, and the scaled velocity is doubled. By studying real dragonfly behavior, other researchers have derived a range of Reynolds numbers over which dragonflies operate. Other researchers have found Reynolds numbers over which micro-aerial-vehicles (MAVs) typically operate. Typical dragonfly chord based Reynolds numbers are in the range of about $10^3 – 10^{3.8}$ (May, 332), while chord Reynolds numbers for MAVs range from $10^4 – 10^5$ (Tamai, 2). Since the Reynolds number for this design is just above 10^4, decreasing the Reynolds number should not have a serious impact on the performance, especially since most dragonflies have Reynolds numbers below this. Decreasing the Reynolds number will allow slower flapping, slower speed, lower weight, and ultimately less power. It would seem silly to make a dragonfly heavier simply to achieve dynamic similarity when other dragonflies of lower Reynolds numbers are quite capable fliers.

The Reynolds number was therefore set as an independent variable with certain constraints above and below according to the Reynolds numbers observed on real dragonflies and MAVs. Using a preliminary SolidWorks model of the scaled down dragonfly with motors, gears, wings, body and tail, a mass was calculated. By varying the Reynolds number of the scaled design, it was possible to optimize the weight to fit the SolidWorks model. The weight of the SolidWorks model was about 10 grams-force which resulted in a Reynolds number of about 7278 or $10^{3.86}$. This is well within the acceptable range indicated by physical experiments with dragonflies. With this change, all of the other design specifications changed besides the wing and chord lengths. The column of Table 1 titled “Modified Scaled Design” shows the new values, many of which are much more realistic than those for the “Scaled Design”.

As a preliminary test of these principles, the WowWee model was partially disassembled, and the wings were cut down using a pair of scissors. Cutting down the wings decreases the torque on the motor, which should affect an increase in the frequency. This was observed but not to as great an extent as expected. Disassembling the dragonfly and removing various non-essential parts reduced the weight.

The resulting cut down model flew but not nearly as well as the original model. It was more stable, and did not have any tendency to stall. It could not maintain level flight and dropped 6 feet vertically over a 2.0 second flight while traveling 12 feet horizontally. Its un-powered flight from an altitude of 9 feet lasted 1.0 seconds, and it covered 8 horizontal feet in that time. Table 3 shows four sets of characteristics. The first column contains characteristics of the original WowWee model, while the characteristics of the cut down model appear in the second column.

Model	Original WowWee	Cut down WowWee	Scaled	Modified Scaled
Wing span (m)	0.413	0.214	0.207	0.207
Wing Chord (m)	0.081	0.070	0.040	0.040
Wing area (m)	0.0167	0.00749	0.00417	0.00417
Overall mass (g)	23.7	15.6	23.7	11.0
Freq (Hz)	9.45	11.35	37.80	25.76
flight speed (m/s)	2.1	1.6	4.2	2.9
Chord Re	11 181	7 460	11 181	7621
Lift Coefficient	5.24	13.01	5.24	5.24
Strouhal No	0.362	0.492	0.362	0.362
Power required (W)	0.45	0.18	0.90	0.28

Table 1: Characteristics of all models

Because the flight of the cut down dragonfly did not satisfactorily match the flight of the original WowWee model, it was hypothesized that the difference was simply weight. To test this hypothesis, weights were added to the original model just above the center of gravity. These weights were various coins, and were inserted between the foam shell of the body and the plastic supporting the wings. The flight of this weighted model became much more similar to the flight of the cut down model, giving good indication that the only difference between the two was weight, and that the coefficient of lift of the cut down model would need to be higher to produce the same flight. This may be seen from Table 3. Likely the coefficient of lift listed is not accurate, because the model could not sustain flight, and is actually lower than the listed value, leading to this unsustainability.

5. Design of and modifications to the half-scale prototype

5.1 Design overview

The physical design of the scaled prototype was completed using the design parameters found from the scaling analysis for the "Modified Scaled Design" in Table 1, and it was done concurrently with that analysis. Designing these two things simultaneously allowed some feedback from SolidWorks to the weight of the design which allowed educated variation of the Reynolds number to fit this weight. Parts were found on various websites and were integrated into the design. Later, when the parts desired were not available, the design changed to accommodate the parts that could be purchased. Once a prototype was built and tested, certain problems were solved by changing the design of some components and remanufacturing them. Figure 5 shows the

preliminary SolidWorks design, while Figures 6a and b show how that design was modified when the parts in Figure 5 were not available.

After manufacture and preliminary testing, certain problems with the design became obvious. The most obvious problems with the original prototype were examined and remedied first with little knowledge of the dynamics. Once these obvious problems were fixed, a model of the dynamics was made to help determine further necessary modifications, and those modifications were made.

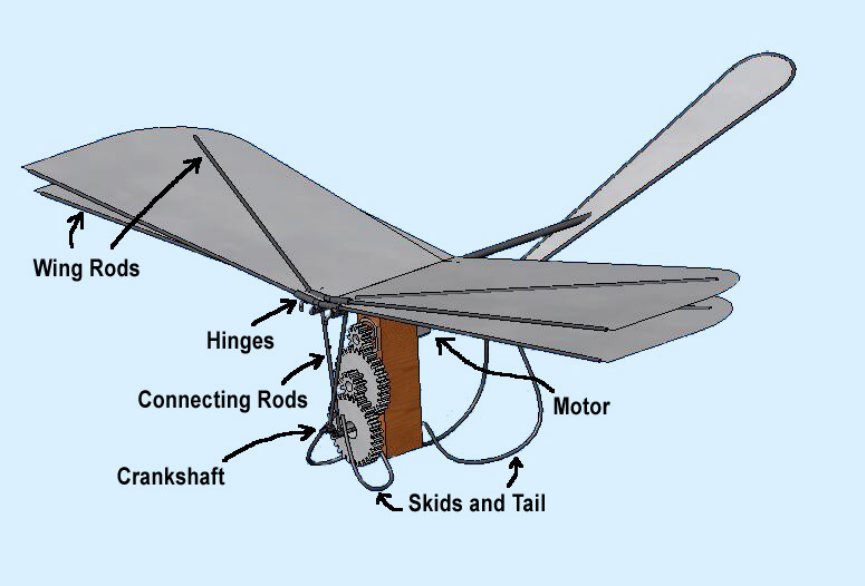

Figure 5: SolidWorks Model 1

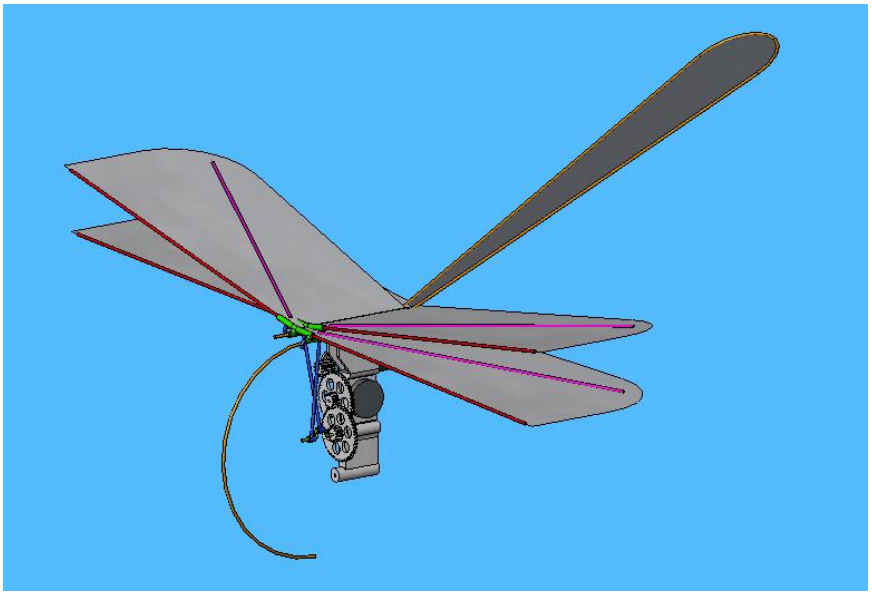

Figure 6a: Overall view of SolidWorks model 2

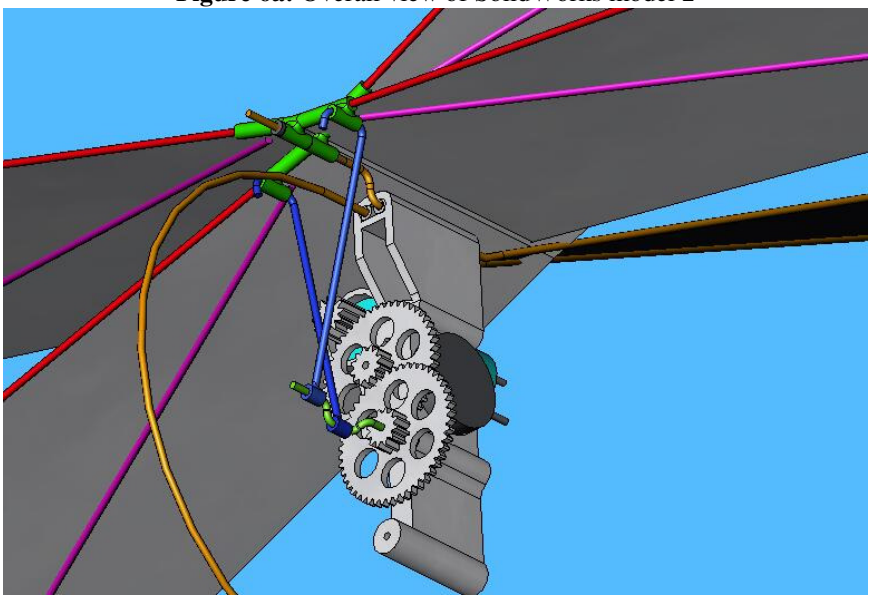

Figure 6b: Detailed view of motor, gearbox and hinges

5.2 Body and frame

Initially, a balsa wood body was modeled in SolidWorks to hold the motor, gears, and wires for skids and tail. The tail and skids were made using a single spring grade stainless steel wire with a diameter of 0.029 inches. This wire was intended to be rigid to a point and then springy if too large a load was applied that might otherwise break the

dragonfly. It was also purchased with some of the other components in mind. This design may be seen in Figure 5.

When the gears and motor were not found however, a full gearbox was purchased instead. The body of this was made of plastic and specially formed to fit the motor and gears it contained. Once received, it was evident that it had been manufactured using a rapid prototyping process, and, considering the availability of the school's rapid prototyping machine to me, this became even a better option should I need to remake this part. This gearbox had two mounting holes near the top as can be seen in Figure 6b. When inserted through these holes, the wire used for the frame could simultaneously be used to create the pin on which the wings rotated. This greatly simplified the design and manufacture as the motor and gears were replaced and the wires had a simpler configuration. This new model can be seen in Figures 6a and b.

5.3 Motors and gearing

Since one major factor of the design is weight, small and light parts were used in the design. Another significant parameter however in choosing a motor was the amount of power available from such a motor. After searching for a motor with low enough weight and high enough power within a desired frequency range, a model was selected which was ultimately not available for purchase. Another significant consideration in the design was the flapping frequency. This was directly controlled by the motor and gearing, and once a motor was purchased, an approximate gear ratio was known. Small gears however are very hard to find and few companies carried gears of the right sizes. One company that did have some selection of miniature gears was Stock Drive Products/Sterling Instrument (SDP/SI), although even their selection was limited.

The best overall option came from a company called The Ornithopter Zone that specializes in flapping wing MAV's for hobbyists, and who sold the integrated motor/gearbox unit described earlier. This resolved the issue of finding an appropriate motor and gears to fit it and reduce the frequency. The gearbox when received had a maximum frequency of 5 Hz, but luckily the last gear in the gear train had a ratio of 12:60. So the second to last gear had the rotational speed required and the crankshaft was inserted into this gear.

To secure the crankshaft in place and attach it securely to the appropriate gear, a few methods were tried. First, Crazyglue® was used, but within a few seconds of operation this had broken off. Loctite® was also tried but to little success. For a time, the joint was held simply by melting slightly the plastic of the gear around the crankshaft so that any gaps were filled. When the crankshaft was moved however as part of another modification, this method failed to work again, and epoxy was used in its place. Since the first bend in the crank is touching the gear, the geometry of this bend was used secure it in place against the face of the gear with the epoxy.

The motor in the gearbox was a seven millimeter diameter brushed DC motor, and the battery was a small coin cell. Both of these components were modeled in SolidWorks of aluminum, and cut outs were made until the modeled weight matched the actual weight of each component. The resulting model is shown in Figure 6.

5.4 The linkage

The four bar linkage of the WowWee dragonfly was replicated on a smaller scale in the scaled design, but the components and manufacturing techniques were changed. Initially, all of the components were made of stainless steel from two kinds of stock

material. The same type of stainless steel wire used for the frame and tail of the dragonfly was used in conjunction with thin tubing with an inner diameter of 0.035 inches and wall thickness of 0.008 inches. This inner diameter was six thousandths of an inch larger than the outer diameter of the 0.029 inch diameter wire. In some components a combination of wire and tubing were used, and any connection between subcomponents was done using solder. These connections were modeled in SolidWorks using fillets.

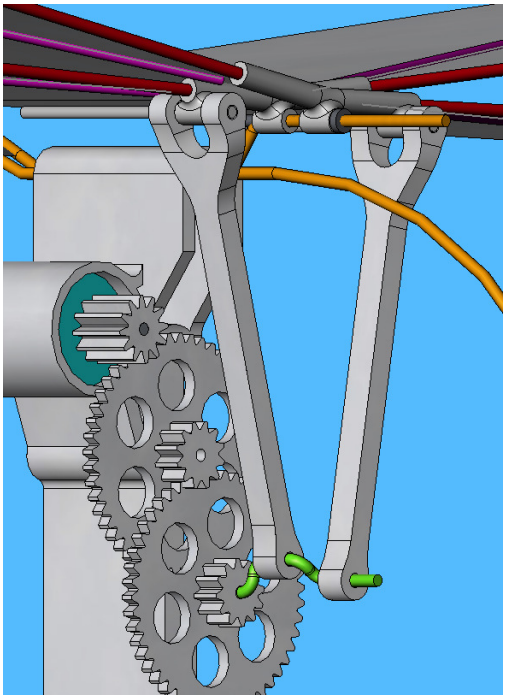

Figure 7: The gearing and linkage in final form

Three parts for this four bar linkage needed manufacture while the body served as the fourth. The first such part was the crank. The crank was designed as a single bent piece of wire. A long straight section was inserted through the last gear and the gearbox, but immediately upon leaving contact with that gear the wire was bent using an offset to create the first of the two cranks. A second offset bend was used to make the second crank on the shaft. This crank is shown in green near the bottom of Figure 7.

The connecting rods, which attach to the crank, went through several iterations before arriving at a final design. Initially, the connecting rods were formed by bending a wire with a right angle, cutting off the excess length, and soldering a very short section of tubing to the end again at a right angle (see Figure 8). The tube at the bottom of the rod fit over the crank while the horizontal wire at the top of the rod fit through a hole in the wing hinge. After continuing testing, the connecting rods between the crank and the wings bent slightly at the solder joint, and oftentimes the connecting rod got stuck on the bends in the crank. Because the fit was so tight between the small tube at the base of the connecting rod and the wire in the crank around which it rotated, any bend in the crank caused the tube in the connecting rod to bind. Very often, even the bends at each end of the crank were enough to cause this binding, and the motor could not break free. When this binding occurred, the solder joints in the connecting rod were stressed, and eventually led to repeated failures. To fix both these problems, plastic connecting rods were made using the school's rapid prototype machine. With holes drilled in the bottom and top of these rods, they slid loosely onto the crank (with no alterations to the crank) and provided good performance without solder joints. In the top, these rods were attached to the wing using a simple pin joint. Unfortunately, the wing hinge and the connecting rod tended to separate during testing. A second iteration of the connecting rods was prototyped which incorporated a small Y at the top of the rod to be pinned to both sides of the wing hinge as is shown in Figure 8. This held the wing much steadier compared to the connecting rod, and so far there have been no failures of this system.

Figure 8: 1st generation connecting rod

The wing hinge, also seen in Figure 8, is a longer section of the same tubing as was used in the connecting rod. It was bent at the middle to allow the wings to have a slight upward angle when closed. Two small sections of the tubing were then soldered on the bottom of and at a right angle to the main section. One was located in the middle to make an axis for the wing, while the other was located a short distance away to make a hole through which the top section of the connecting rod could pass. This design was not modified throughout the design process and still works well.

One significant modification to the linkage was the shorting of both the crank and the pin on which the hinges rotated. An analytical model (described later) was created to analyze the linkage and showed that as these wires were shortened, the wing motion improved dramatically. During this process, a new crank was required which was made out of the same wire as the rest of the wire components instead of the provided shaft wire that came with the gearbox.

5.5 The wings

Initially, wings were designed with the same shape as those of the WowWee dragonfly but with each dimension half of the original. The first generation wings were made of the material from a grocery bag which was the same thickness as the material used in the WowWee model. After some very preliminary testing showed that these wings were not adequate, the wing material was changed to polyester film. This material was chosen after examining the wings on a remote control airplane and comparing them to the wings of the WowWee model. The wings of the plane were known to be made of polyester film, and they appeared to be the same material as the wings of the WowWee

model. This material had the same thickness as the grocery bags, but was more smooth, flexible and less likely to crease making it more suitable to the application.

The wing rods at the leading edge and along the diagonal of each wing were placed according to the placement in the WowWee model. These can be seen in Figures 5 and 6. Initially these rods were made from the same wire as the linkages, tail and frame until this material proved too massive. To decrease the mass of these rods, carbon fiber composite wire was used instead. Carbon fiber composite just sinks in water indicating that it has a density about one seventh that of steel (Beer, 747). Substituting carbon fiber rods into the wings instead of steel rods (of the same geometry) created wings that were about one third the original mass.

5.6 The battery

Since this MAV will fly using electric power, a battery was chosen to directly power the motor. Initially, a 3.0 Volt alkaline coin cell was chosen with weight being a major deciding factor along with voltage and energy storage capacity. Although this voltage was enough to produce a flapping frequency of 24 Hz, a simple first test with the battery however showed that the current capacity of the battery was much too low for the motor's needs. To remedy this problem, the battery from the WowWee model was studied and determined to be a 3.7 Volt lithium polymer battery. Lithium polymer batteries are rechargeable and light weight, and they have a very low internal resistance (approximately 1 ohm). The higher voltage of these batteries also allows for increased frequency if necessary. The energy stored by these batteries, though not as important, is within an acceptable range allowing for extended flight. A battery with lower capacity

and weight was purchased from the same company as made the battery for the WowWee model, and has performed well since.

5.7 Summary of design and modifications

The overall design of the half scale prototype is very similar to that of the WowWee model, but each of the parts has been scaled down. Some modifications were made the design to allow for easier manufacture with the tools available, and some further modifications were made once certain components did not work as well as planned. This process took place in a step by step fashion where one modification was followed by testing and then another modification. Although slow, this allowed for evaluation of each modification individually.

6. Manufacture of the scaled prototype

Although the design of the scaled prototype is fairly simple, actually manufacturing the components proved difficult. First the hinges (shown in Figure 6b in green or in Figure 7) were created. The tubes were bent the required 10 degrees using two pairs of pliers, then the smaller tubes serving as hinges were soldered on. However, stainless steel does not solder easily, so liquid flux was used to clean and prepare the surfaces. It was most effective to solder the pieces together while they were submerged in a droplet of flux which vaporized on contact with the soldering iron tip. The distance between the small tubes on the hinge component was critical so a fixture was created out of a small piece of aluminum sheet metal. See Figure 9. This fixture had two small holes drilled at the

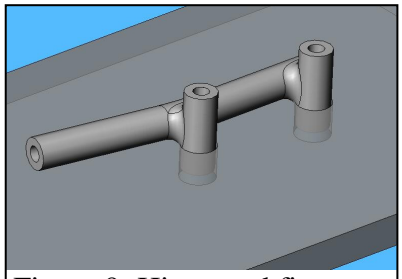

Figure 9: Hinge and fixture

required distance of these tubes such that the tubes could be inserted, the main tube laid across them, and the two solder joints made effectively. This worked well. The aluminum material of the fixture proved important because the solder did not stick to the aluminum even with flux, and the hinge component could be easily removed when completed.

To create the first generation connecting rod, a piece of wire was bent at a right angle and cut to length. A small piece of the tubing was also cut and the two were soldered together. Because the length of this component was again critical, two additional holes were created in the aluminum fixture (see Figure 10) with diameters of 0.034 inches, and separated by the required length of the connecting rod. The end of the connecting rod not to be soldered was inserted through one hole while a small scrap piece of the same wire was inserted into the other hole and the small tube fit onto that. This located both the connecting rod and the tube, and the two could be soldered together with precise positioning.

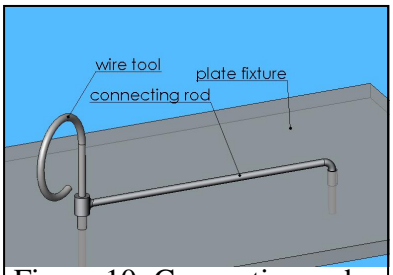

Figure 10: Connecting rod, tool, and fixture

The second and third generation connecting rods were made using the school's rapid prototype machine. Creation of these components was fully automatic, and the rapid prototype machine printed accurately made parts. Typically however the holes on these connecting rods were too small, and a small drill was used in a drill press to enlarge these. The hole to fit over the crank was enlarged much to allow it to fit over and around the bends of the crank. The hole used at the top to connect to the wing hinge was enlarged to just larger than the size of the wire pin to be used.

To create the crank, an offset bend as described in Section 5.4 was needed. This bend required an offset between the two wire centers of 0.080 inches. Needle nose pliers

were too large to create this, and any other existing devices could not create the sharp corners necessary. To create this part, a new fixture was created which acted to stamp this bend into the wire much like an offset bender for tubing. Since an eighty thousandths bend was needed in spring steel, this tool was made to bend ninety thousandths after which the wire would spring back to the required dimension. This tool was created by cutting a block of steel (aluminum was tried first but was too soft) in half and milling flat the two cut faces. All but 0.090 inches of the flat face of one of the halves was milled down 0.090 inches, and 0.125 inches of the other half was milled down the same 0.090 inches so that when put together the pieces fit like puzzle pieces and looked like a whole. The space left between the two halves horizontally was intended to allow the wire a place to go to prevent cutting by shear. This fixture is shown in Figure 11. Holes were drilled in each half in corresponding locations, such that when a pin was press fit into one half it would slide in the other and the two halves could be pressed together and separated without any transverse movement. When a wire was placed between the halves, and the halves were squeezed together using a vice, the wire was bent with an offset very nearly the required 0.080 inches. To create the crank, this process was repeated twice with the first bend placed just outside the tool so that the second offset bend would be close to the first.

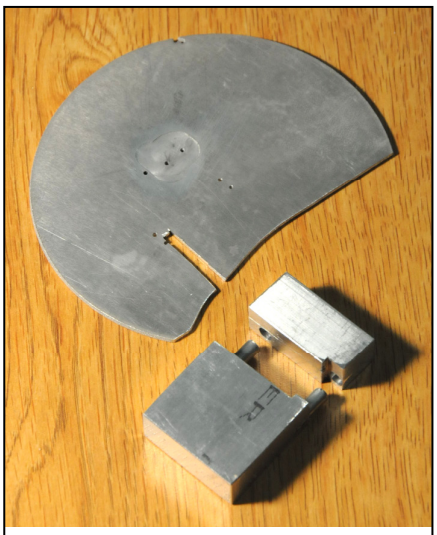

Figure 11: Fixtures used in manufacture

Because the first generation connecting rod could not slide on the crankshaft past the bends created, one bend was created, one of the connecting rods was slid onto the

shaft, and finally the other bend was created around the connecting rod. The tube in the connecting rod in this process was placed between the halves of the offset bending tool, but when no other forces were exerted on it the connecting rod (particularly its solder joints) stayed intact throughout the process. If there was any breakage of the solder joint during this operation, a soldering iron was used to re-melt the solder and make the connection secure again using the fixture for this process. To insert the crankshaft into the fixture for this re-solder operation, a slot was cut which intersected the hole which the scrap wire from the original manufacture had been placed through. Because the crankshaft was bent, it did not simply slide through the original hole and this slot was necessary for insertion and removal.

The tail of the scaled prototype dragonfly was created by bending a two foot long wire roughly in half with a large radius of curvature. The two ends of the wire were then inserted into the holes in the gearbox (as shown in Figure 6b) and the wires were soldered together on the tail side of the gearbox. This ensured that the tail did not twist excessively. Finally the wires were bent as is shown in Figures 6a and b using pliers and fingers. These last bends were not precise except the one used to position the hinges.

The gearbox purchased also required modification. The frequency of the output shaft was about five times too low, To modify it, the last two gears were removed and the second to last hole was enlarged to accept the output shaft. The included output shaft was bent to make the crank and inserted into the second to last gear and the corresponding hole. The gear was secured on the crankshaft using superglue. When the superglue broke during testing, the plastic gear was melted using a soldering iron and formed a good bond to the crankshaft. When further failures occurred after modification, epoxy was used.

The wings and tail surfaces were created using plastic from a grocery bag of thickness 0.0005 inches. This was the same thickness as the wings from the original WowWee model. These plastic sheets were secured to their respective wires using strips of Scotch® brand tape that were cut to be $^{3}/_{16}$ of an inch wide.

The final result of the manufacture before modification is shown in Figure 12.

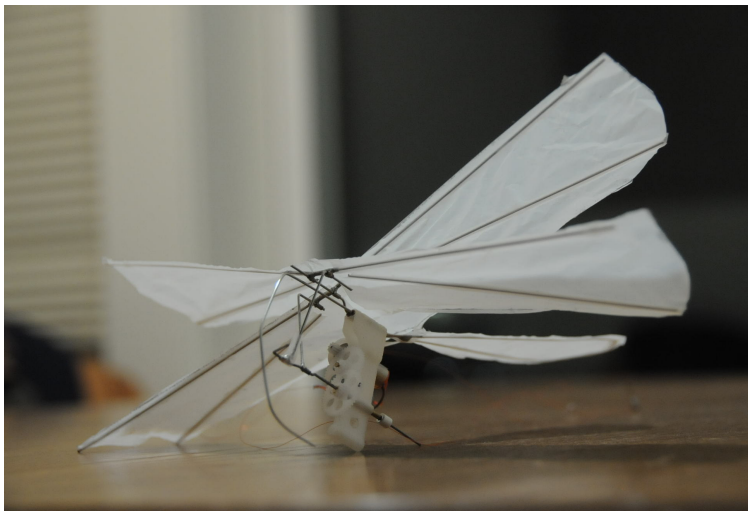

Figure 12: The 1st generation scaled prototype

7. Testing and results of the scaled prototype

7.1 Testing overview

Testing of the prototype was done as a step by step process alongside modification. Each modification was the result of a test, and after each modification, a test was done to evaluate the change. The following sections describe each test and what modification each evaluated.

7.2 Preliminary and battery testing

Preliminary testing was done first by hand, then by using the battery, and finally by using a power supply. With hand testing, the prototype worked great. The wings

separated and came together nicely, and there were no problems. This showed that the prototype was made with sufficient precision and was ready to be tested electrically.

Testing using the coin cell battery was done by placing the leads of the motor wires in contact with the terminals. The motor turned, and the prototype flapped successfully. However the flapping frequency was about 4 or 5 Hz, much lower than what it should have been, and over the course of thirty seconds the frequency slowed further. This showed that the battery was likely not powerful enough to run the motor. The motor could take a maximum of 3.7 V DC input, and the batteries used were tested to be 3.2 V but rated at 3.0 V. After running the motor using the battery for about 30 seconds, the battery was again tested and the voltage was found to have dropped to about 2.7V.

When the lithium polymer battery was connected, the prototype flapped very quickly. When not connected, the battery had a voltage of 3.8 V, and when connected to the motor that voltage dropped to 3.6 V. This showed the current capabilities of this battery and that low frequency would not be a problem caused by the battery. This battery can power the prototype at full speed for about a minute.

7.3 The frequency response to voltage

By using a power supply, and connecting everything using a breadboard, the voltage across the motor could be varied and monitored precisely. Even a very low voltage produced a flapping motion that was as fast as that produced with the battery. Further tests were done using a strobe tachometer to measure frequency. Flapping frequency, current, and power were recorded for several voltages.

First, this data was collected for the gearbox alone without any other mechanisms or wings attached to it. From the cut down dragonfly, it is reasonable to assume that adding

wings will decrease the frequency somewhat but not dramatically enough to cause the prototype not to fly. This hypothesis was tested by adding the grocery bag and stainless steel wings. Although an extensive analysis was not yet carried out, the flapping frequency at 3.0 V was 20.1 Hz, slightly below the frequency without wings. When at this setting, I placed my hand behind the dragonfly to feel the wind produced. Although there was some wind produced it did not feel like enough to let the prototype fly.

These wings behaved fine at low frequencies, but as the frequency increased the power increased much more dramatically and the dragonfly seemed as though it would break apart. To remedy this, the carbon fiber wing rods were substituted in place of the steel. Further testing was done to analyze the effect of this change, and the results from these frequency vs. voltage tests in the various configurations – with and without wings, carbon fiber or steel rods or no wings at all – showed that the impact of this change to carbon fiber was significant (see Figure 13). Although there was still a slight decrease in the frequency from no wings to carbon fiber wing rods, that decrease was much less pronounced than the decrease from no wings to steel wing rods with polyester wings. The steel wing rods with polyester wings had a maximum measured frequency of just over 7 Hz while the carbon fiber wing's frequency increased with increasing voltage for all voltage tested (maximum of ~25Hz tested). No data was taken for the steel wing rods with grocery bag airfoils.

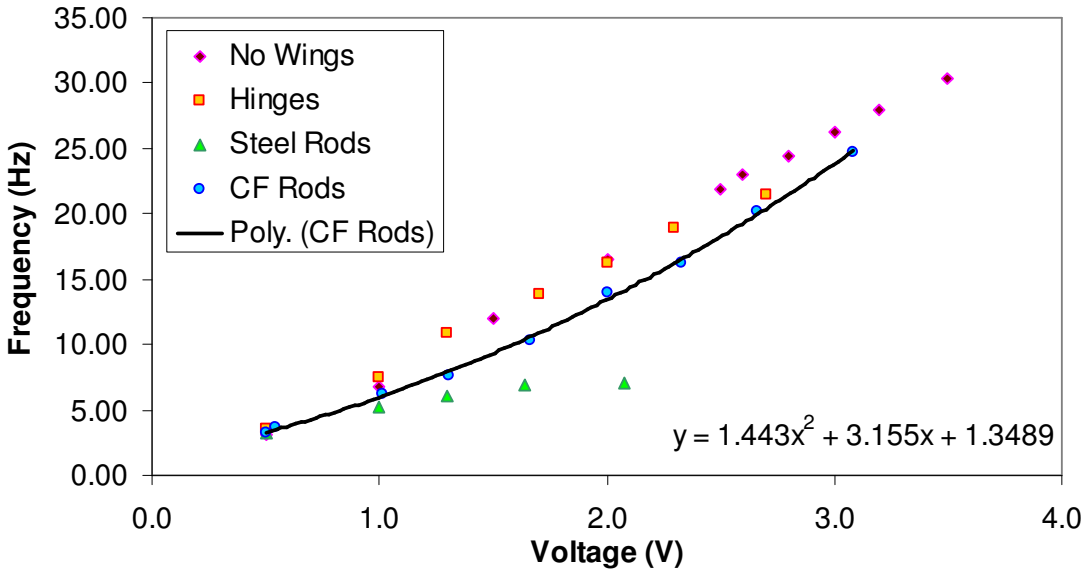

Figure 13: The affect of wing mass on frequency

7.4 Flapping symmetry

If the first generation prototype was held by hand during testing with the wings were attached, significant horizontal vibration could be felt. Since this only happened when the wing airfoils were attached, the forces causing the vibration were likely due to the unsteady aerodynamics at work which were not completely balanced on each wing. When the motion was slowed down and analyzed using either the camera technique described in Section 3 or when the gears were turned by hand, it became evident that there was some side to side rocking; the wings closed, came together, rotated together a few degrees passing through horizontal, and then opened again a few degrees off horizontal. This motion was repeated when the wings were fully open but was not as obvious. This motion can be seen in a short series of pictures in Figure 14 (especially the 5th and 6th images) or in a longer series in Appendix E which describes the characteristics designed and measured for the scaled prototype. Any motion where the wings are not

flapping symmetrically about the vertical “right” plane will cause significant vibrations beyond those expected for normal flapping.

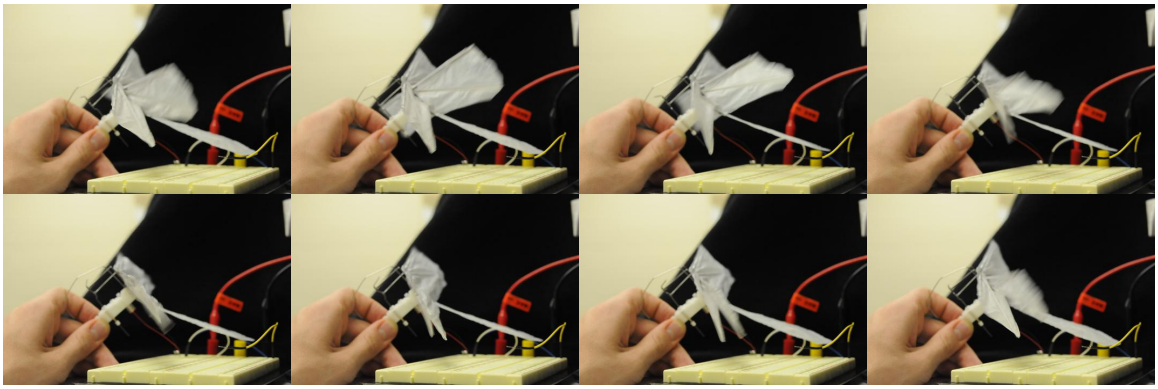

Figure 14: Asymmetrical flapping of 1st generation scaled prototype

After the crank geometry was adjusted slightly, the wings became much more symmetrical. Although some vibration was still evident, the frequency could be easily increased much past the prior limit where fear of destroying the prototype limited it.

7.5 Airfoil testing

Another problem with the motion of the first generation prototype was the shape of the deformed airfoil when flapping. For stable flight, all the airfoils should deform in the same way, and this deformation should mimic the deformation of the airfoils in the WowWee model. Neither of these criteria was met. The wings all deformed slightly differently, and some deformed more on the up stroke and others more on the down stroke. Also, although this deformation was similar in overall shape to that of the flapping WowWee model, each wing deformed a different amount than the WowWee model. This, even more than the asymmetry of the flapping, is likely responsible for the lack of propulsive force felt.

When the wing material was changed to polyester, the wings deformed much more easily and consistently, and to a better degree they mimicked the deformations in the

WowWee wings. Although this increased deformation is expected to have created more thrust, a quantitative test was unfortunately not completed to evaluate this change. Some problems arose around slack in the airfoil near the body and the trailing edge of the wings. This slack likely caused some lack of lift due to unchecked deformation of that part of the wing, but this problem has not yet been resolved.

7.6 The flapping angle response to frequency

It was observed in various tests that as the frequency of the wings increased, the amplitude with which they flapped decreased dramatically. At high frequencies, the wings just twitched and little thrust was produced. This can be seen in Figure 15. This problem was most pronounced when using the first generation rapid prototyped connecting rods, because in this case the pin connecting the rod to the wing hinge was loose and was getting pushed around with very little force. This was corrected with the Y shaped connecting rods. Data linking the flapping amplitude to frequency was taken at several frequencies, and a plot of this data appears in dark blue in Figure 16

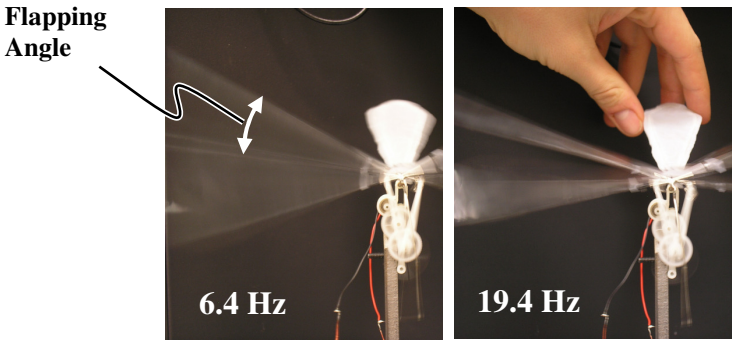

(a) (b)

Figure 15: The affect of frequency on flapping angle

After a new and shorter crank and hinge pin were made, the wings were much more resistant to the decreasing flapping amplitude that they experienced before at high frequency. After epoxying the crank to the gear that turned it, so that the crank would not

slip in the gear, a second set of data was taken. This new data from the modified prototype appears alongside the original data in Figure 16. It can be seen from this data that the flapping angle becomes independent of the frequency after accounting for measurement error. It may also be noted that the average flapping angle increased to about 42 degrees, although the reason for that has yet to be determined.

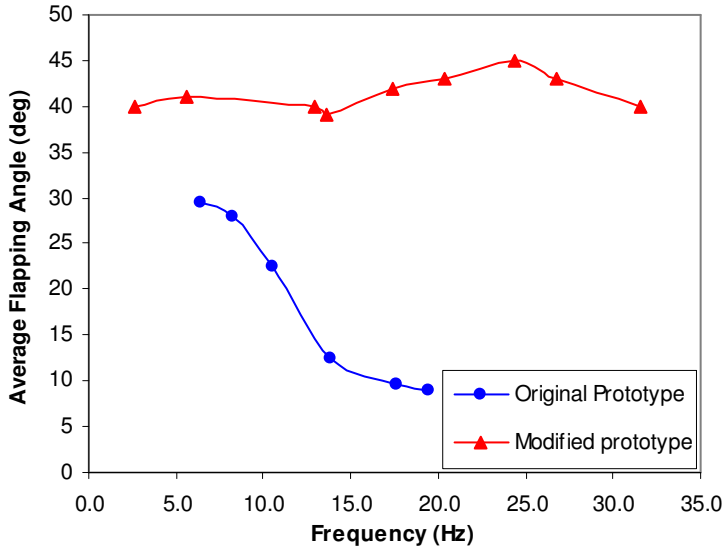

Figure 16: Effect of modifications on average flapping angle

7.7 Final result

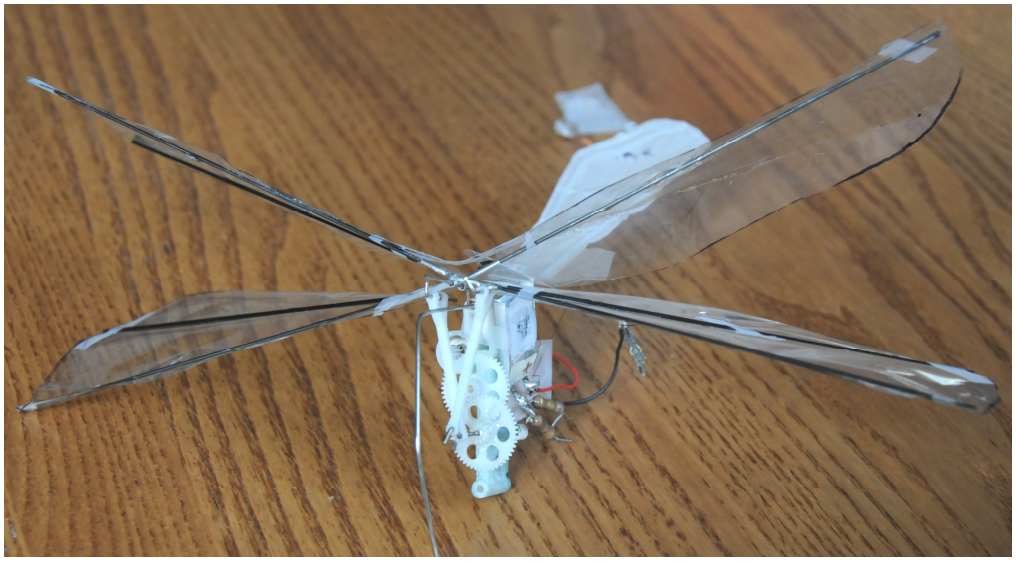

Figure 17: Final Prototype

Figure 17 shows the final prototype after all testing and modification was complete. Although the prototype did not fly as successfully as was desired, it had the same characteristics as the original WowWee model and was very nearly half the original size. The scaling analysis showed that the prototype has those characteristics that should allow it to fly. The weight of the prototype with the battery, wiring and motor and all other components is 11.0 grams, very slightly below the original target weight. The flapping angle of roughly 42 degrees matches the flapping angle of the original WowWee design, and the wings have a similar shape. One difference between the WowWee model and the scaled prototype is the stiffness of the wings. The WowWee model has relatively stiff wings that fit well onto the body and are not slack at any point. The scaled prototype's wings have a less tight fit, and there are places where the wings are slack and likely provide little lift. Other possible differences between the models include the locations of the center of lift, center of mass and center of drag. These and possible other differences combine to influence the aerodynamics and flight characteristics of the prototype.

In its initial flight test, the prototype showed signs of both lift and thrust, but did not fly. After analyzing how much resistance to put in series with the battery to reduce the voltage across the motor and thus the speed, all components were attached to the gearbox of the dragonfly. A small switch was created when a connector was attached to the free lead of a resistor whose other end was attached to the battery. When turned on and gently tossed by hand, the dragonfly first dropped before leveling out at a (very approximate) downward 45 degree angle. Thrust was demonstrated when the dragonfly moved forward, and lift was demonstrated when it did not tumble but instead stayed upright. When fixed in a position and powered, it is clear to any hand placed behind the wings that a significant amount of thrust was created.

The other significant achievement was the creation of the analytical model. The model predicted with some accuracy how changing various parameters or dimensions would effect changes in the flight of the dragonfly. As compared with experimental data, the model predicted roughly the same changes in characteristics with modifications in the various cases which it could distinguish. This model is described in Section 8.

8. Creation of an Analytical Model

8.1 Model Overview

In Figure 16 in section 7.6, we see a blue “Original Prototype” curve that looks distinctly like a low pass filter. From intuition we know that as the frequency or flapping angle increases the power also increases, and that physical systems will always choose the option which uses the least power. Therefore we see that at low frequencies the power output is small but at higher frequencies when the power output does not want to

increase, something must give, and that which gives is the flapping angle. That short analysis is useless however at telling us how to fix the problem. In order to be able to better analyze how certain factors influence the flapping amplitude at high frequency, a computerized model using the Matlab software package was made, tested and used to model the prototype.

The overall idea of the model is that the linkage is modeled from which aerodynamic and inertial forces are found which contribute to a deflection analysis which is fed back into the linkages model. Iterating this several times at each position of the wings and crank allows a precise solution of where the wing is. Comparing the maximum wing angle to the minimum determines the flapping angle for a given frequency. Incrementing again over multiple frequencies allows the curve in Figure 16 to be replicated by the program.

8.2 Positions and time derivatives of the linkage

The first step in the analysis is finding the position of the linkages in the system. For ease of modeling, only one linkage was modeled. Figure 18 shows how the links were set up for analysis. Equations 7 – 10 describe the positions of each point in the linkage. *P* represents the position of the point in [*x*,*y*] indicated by its subscript, while *L* represents the length of the specified link. θ represents the angle of the specified link with respect to the horizontal.

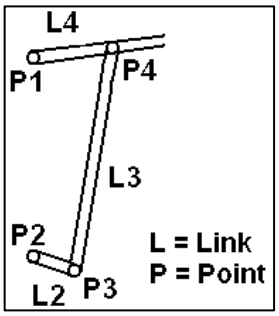

Figure 18: Link names

$$P_1 = [0,0] \tag{7}$$

$$P_2 = P_1 + [0,-L_1] \tag{8}$$

$$P_3 = P_2 + [\cos\theta_2, \sin\theta_2] \tag{9}$$

$$P_4 = \left[a + b \cdot \frac{-d \pm \sqrt{d^2 - 4 \cdot c \cdot e}}{2 \cdot c}, \frac{-d \pm \sqrt{d^2 - 4 \cdot c \cdot e}}{2 \cdot c} \right] \tag{10}$$

$$a = \frac{{P_{3x}}^2 + {P_{3y}}^2 - {P_{1x}}^2 - {P_{1y}}^2 - {L_3}^2 + {L_4}^2}{2 \cdot P_{3x} - 2 \cdot P_{1x}} \tag{10a}$$

$$b = \frac{P_{1y} - P_{3y}}{P_{3x} - P_{1x}} \tag{10b}$$

$$c = b^2 + 1 \tag{10c}$$

$$d = 2 \cdot a \cdot b - 2 \cdot b \cdot P_{3x} - 2 \cdot P_{3y} \tag{10d}$$

$$e = a^2 - 2 \cdot a \cdot P_{3x} + {P_{3x}}^2 + {P_{3y}}^2 - {L_3}^2 \tag{10e}$$

After modeling the positions of each of the joints and links, the velocities and accelerations were calculated for links 3 and 4 based on an input velocity of link 2. The angular velocity of a link is denoted by $\dot{\theta}$ while the angular acceleration is denoted by $\ddot{\theta}$.

$$\dot{\theta}_4 = \frac{L_2 \cdot \dot{\theta}_2 \cdot \sin\theta_2 - L_2 \cdot \dot{\theta}_2 \cdot \cos\theta_2 \cdot \tan\theta_3}{-L_4 \cdot \sin\theta_4 \left(1 - \frac{\tan\theta_3}{\tan\theta_3} \right)} \tag{11}$$

$$\dot{\theta}_3 = \frac{L_2 \cdot \dot{\theta}_2 \cdot \cos\theta_2 - L_4 \cdot \dot{\theta}_4 \cdot \cos\theta_4}{-L_3 \cdot \cos\theta_3} \tag{12}$$

$$\ddot{\theta}_4 = \frac{a - \tan\theta_3 \cdot b}{-L_4 \cdot \sin\theta_4 \left(1 - \frac{\tan\theta_3}{\tan\theta_4} \right)} \tag{13}$$

$$\ddot{\theta}_3 = \frac{b + L_4 \cdot \cos\theta_4 \cdot \ddot{\theta}_4}{-L_3 \cdot \cos\theta_3} \tag{14}$$

$$a = L_2 \cdot \cos\theta_2 \cdot {\dot{\theta}_2}^2 + L_2 \cdot \sin\theta_2 \cdot \ddot{\theta}_2 + L_3 \cdot \cos\theta_3 \cdot {\dot{\theta}_3}^2 + L_4 \cdot \cos\theta_4 \cdot {\dot{\theta}_4}^2 \tag{13,14a}$$

$$b = -L_2 \cdot \sin\theta_2 \cdot {\dot{\theta}_2}^2 + L_2 \cdot \cos\theta_2 \cdot \ddot{\theta}_2 - L_3 \cdot \sin\theta_3 \cdot {\dot{\theta}_3}^2 - L_4 \cdot \sin\theta_4 \cdot {\dot{\theta}_4}^2 \tag{13,14b}$$

8.3 Moments on the wings

After the linkages were analyzed, the moments on each wing needed to be analyzed about the axis of rotation. The inertial moment is calculated first for a single wing. In equation 15, ρ_{cf} is the density of carbon fiber composite wing rod, while r_{cf} is its radius. L is the wing length.

$$M_{inertial} = \rho_{cf} \cdot \pi \cdot r_{cf}^{\,2} \cdot \tfrac{1}{3} L^3 \cdot \ddot{\theta}_4 \tag{15}$$

The aerodynamic moment is more complicated to calculate. Since the aerodynamic moment calculation uses a drag coefficient of the wings traveling vertically through the air, a drag coefficient was calculated using Cosmos FloWorks with SolidWorks. Many thin airfoil geometries were tested to determine their drag coefficient, and it was found that while the curvature of the wing did not significantly impact the drag coefficient, the angle of attack did significantly impact this coefficient. An equation was found which approximated this drag coefficient given an angle of attack using a third order polynomial. In order to find the angle of attack at every point along the length of the wing, an approximation was assumed where the trailing edge of the wing went through the same motion as the leading edge but with a phase shift specified by an input to the program. The program recalled past angles of the wing to determine the angle of the trailing edge of the wing about its axis, and the tilt of the wing was initially calculated as an arctangent of the difference of the height of a point on each edge. However in order to calculate the overall moment created, integration was needed along the length of the wing. Because that integration contains the arctangent of a third order polynomial, it is difficult. It was calculated using an internet version of the Mathematica integration tool, but the output contained a function which was not preprogrammed into Matlab, and I

could not program it. So some approximation was made. It was assumed for simplicity that the wing formed a helix shape going from zero degrees at the center to the maximum angle at the end, which was found using the arctangent function. This approximation is shown graphically in Figure 19.

Figure 19: Tilt modeled with the arctangent (left) or helix (right)

This new function was much easier to integrate, and that integral appears in Equation 16b as part of the calculations for the aerodynamic moment calculated in Equation 16. In these equations, *L* represents the length of the wing, while *W* represents the width from front to back of the wing.

$$M_{aerodynamic} = \tfrac{1}{2} \cdot \rho_{air} \cdot W \cdot \dot{\theta}_4^{\,2} \cdot b \cdot \frac{\dot{\theta}_4}{\left|\dot{\theta}_4\right|} \tag{16}$$

$$a = \frac{1}{L}\tan^{-1}\left(\frac{L}{W}\cdot\sin\theta_4 - \sin\theta_{trailing-edge}\right) \tag{16a}$$

$$b = \frac{0.7925}{7}a^3L^7 - \frac{1.5094}{6}a^2L^6 + \frac{0.0865}{5}aL^5 + \frac{0.8321}{4}L^4 \tag{16b}$$

8.4 Deflections of the wings

By adding these two moments together from equations 15 and 16 and multiplying by the four wings, the total moment that will affect a deflection in the crank could be calculated. Using statics, the moment on the wings could be converted to forces on the crank and the pin wing connector. The deflections for each were then calculated using the following equation 17. *E* is the Young's modulus for the material of which the beam

(crank or hinge pin) is made, while I is the moment of inertia of each beam cross section. L is the length of each beam and F is the force applied to each beam.

$$\Delta y = \frac{L^3 \cdot F}{3 \cdot E \cdot I} \tag{17}$$

Using these equations, deflections in the two members were calculated. These deflections went to update the values of P_1 and P_2 by simple addition. Using iteration (with convergence typically in three to four iterations), an accurate deflection and wing position as functions of the crank position were found. With this crank angle incremented across all positions, a minimum and maximum wing angle could be found. The difference provides the flapping amplitude.

8.5 Results of the analytical model

Tests were run at many frequencies, and Figure 20 shows the result of the analytical model superimposed on the experimental data. Although the model does not precisely predict the curves, it does show some of the same relationships of flapping angle to frequency that the experimental data shows. When some modifications were made to the prototype, similar changes were made to the inputs of the computer model. The results from all four tests (unmodified and modified from the computer model and prototype) were then superimposed in one plot which is shown in Figure 20.

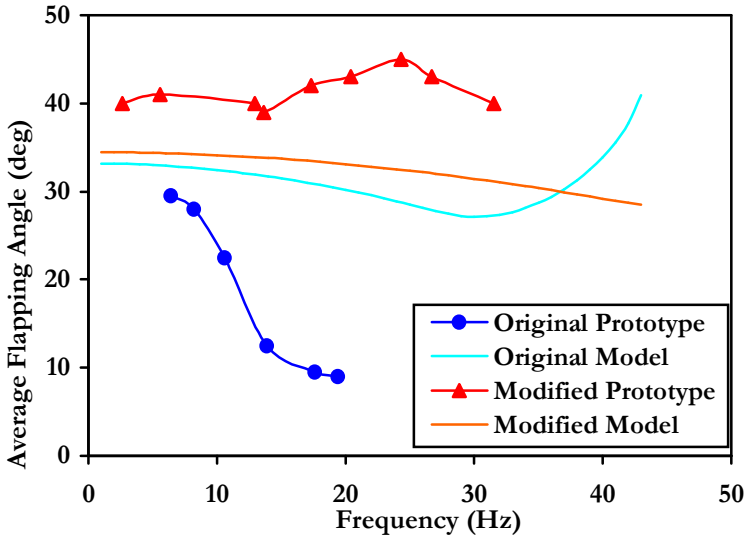

Figure 20: Correlation of analytical model to experimental data

Although the curve representing the behavior of the modified prototype does not follow exactly the curve representing the modified model, the change in shape between the model curves is also reflected in the change in shape between the prototype curves. This indicates that the model did a decent job at approximating the real life prototype. Although the model saw little real use, its creation provided good understanding of which issues were most important for improving the prototype.

9. Conclusions

The major goals of the first term were met, and on time. The only goal that was not met was the continued testing of the scaled prototype which would result in modifications and improvements to allow the prototype to fly. The goals of the second term were not met with as much success. The design was modified to improve the mechanical, electrical and aerodynamic properties of the prototype, but the prototype never successfully flew. The model created as part of the analysis of the mechanics was a partial success due to a

limited understanding of the relevant factors and possibly insufficient testing. The overall goals of the project, including making a flying prototype to test the aerodynamic scaling theory used and designing a new flapping mechanism with the opportunity for further scaling, were again not achieved, though the current prototype is close to being ready for testing against aerodynamic theory. As a next step in the future, further modifications will be made to the prototype to try to approach flight with as much success as possible. If the prototype is successfully able to fly, this will also verify that the scaling theories applied in this design are actually applicable.

One major downside to the mechanisms used on this dragonfly is their scalability. It was very difficult to find parts as small as needed even for this design, and this design only used a scale of one half. If a quarter scale design is desired, a different design of flapping mechanism will need to be created. It is likely easiest to create this flapping mechanism on a larger scale using parts that can be scaled down. The ultimate goal in this specific area of research is to create a robot that mimics a dragonfly in size, maneuverability and control, and has the option to mount a camera for viewing images remotely. Although this goal seems far away, continued research in this area should allow these goals to be met in the future. The WowWee model after all is only four times larger in each dimension than a real dragonfly.

10. Future work

10.1 Overview of future work

Future work on the current prototype will be somewhat manageable, while future work on the project as a whole could be quite extensive while trying to create a robotic

dragonfly of the same dimensions as live ones. For improving the prototype, two elements will be researched. First, the prototype will need further testing and improvement. Second, the analytical model will need further analysis to make sure it is all correct, and to add other features not currently present.

10.2 Future work on the current prototype

Partly due to a lack of time, the aerodynamics of the prototype were not nearly tested to the point they should have been, and it is unknown how the aerodynamic forces act. In order to learn such information, the wind tunnel available on campus can be used to determine both the lift and the drag forces on the prototype at different airspeeds and flapping frequencies. These should be compared to similar measurements or calculations for both the WowWee model, and for the initial target parameters of the scaled prototype. For example, it may be found that the lift forces on the prototype are not nearly as high as they should be, and that further modification to the wings is necessary. In another case, it may be found that the lift and thrust forces are sufficient, in which case another characteristic of the prototype would need modification.

Other such characteristics are the locations of the center of mass, the center of lift, and the center of drag. The center of mass is easily found by hanging the prototype from a string, taking a picture, and extending the line of the string down through the prototype as described for the WowWee model on page 8. The center of lift is more complicated, and can only easily be found by studying the airfoils more closely. However, some trial and error technique can be used by shifting the position of the 0.8 gram battery around and monitoring the performance.

Another parameter that is easily altered is the resistance in series with the battery and the motor. While a potentiometer may be used to select a proper operating frequency when connected to a breadboard, only a fixed resistor is small or light enough to use on the flying prototype. Two such resistors may be seen in Figure 17. Altering the resistance of these resistors can vary the voltage across the motor which alters the motor frequency and thus the flapping frequency anywhere from the maximum possible with the battery of about 30 Hz to zero. The resistors are used to protect the gears and motor from excessive wear.

The shape of the airfoils should also be analyzed or altered to ensure that the airfoils produce the lift required. Currently the slack in the thin airfoils allows them to deform with little force which leads to possible low lift production for the wing area. As can be seen from Figure 17, particularly in the upper right wing in the picture, the wing is loose, and tightening it could provide significant benefits. Finally, the tail is still currently made of a piece of the original grocery bag material which, although it seems to work sufficiently well, could still possibly stand changing. It is possible as well that the size of the tail needs to be changed. The scaling analysis was not completed originally for the tail, except as a general scaling of the entire model by the specified amount. In updating the airfoils, the attachment mechanism of the wings to the body could be modified from the current method involving Scotch® tape, although the tape does work reasonably.

10.3 Future work on the analytical model

In order to continue to help the design of the prototype, work will need to be done on the analytical model both to check the validity of what has been modeled as well as to add new features. Any number of things may have gone wrong during the creation of the

model, and testing should be conducted systematically on each result to verify the results. Further improvements to the model include the addition of code relating to thrust calculations for various situations so that results from wind tunnel testing may be predicted. These improvements will make it easier to understand how various changes will affect the prototype before the change is made.

10.4 Future work and the design of a life size flapping mechanism

Future work on the rest of the overall project could be very extensive. As a first step, further research will need to be done to design a flapping mechanism which can be scaled down at least to if not past the scale at which live dragonflies operate. Some work has been done by researchers at other universities, especially Robert Wood at Harvard University, in creating such flapping mechanisms. His research is a very good place to start to look for answers, and some of his articles are listed here in the references for this current research. Typically the methods used to create such small flapping mechanisms use four bar linkages to magnify the motion of an actuation such as piezoelectrics or electroactive polymers. In these mechanisms, the actuator is connected to the rocker in the four bar linkage, while the wings are connected to the crank. This allows great magnification potential of the motion. The four bar linkage is typically made of folded material where the joints are the folds, and the links are sections of material where the rigidity has been increased. Piezoelectrics have not been used in the papers I have seen to successfully create a flying prototype due to especially the weight and to some degree the size of the housing around the piezoelectric actuator. Electroactive polymers have a better record, and Robert Wood of Harvard has successfully manufactured a prototype capable of lifting its own weight (Technology Review, 2008). Of the two types of electroactive

polymers, the more common is a sandwich of a gel material between two electrodes which act as a capacitor. When a high voltage is applied to the electrodes, the gel is squeezed thin and expands outward allowing an extending action. When the voltage is released, the gel regains its original thickness and contracts lengthwise. A second type of process is one where the material properties of the material, and how the atoms are arranged within the molecules, change when a voltage is applied. These processes happen at much lower voltages than in the first type of actuator, and films have been shown to bend with significant force, displacement and speed. There is little currently written on this technology, but it seems from the designs of the micro flapping mechanisms that the preferred actuator is the second type of electroactive polymer described above.

Other kinds of possible actuation techniques include the use of the first type of electroactive polymer to be used as the equivalent of a muscle to pull the wings to and fro, or the use of very thin shape memory alloy wires to do the same. Shape memory alloy is any one of a number of composite materials which can “remember” a shape and transform to the shape when heated. Such a transformation typically involves the contraction of a long wire. Typically this heating is done electrically, while cooling is done through convection. The nature of the material is such that as the thickness increases, the frequency at which the actuation can repeat itself decreases. While in a dragonfly, convection of the air blowing over the wings is increased from normal, but the wires used would still need to be very thin. Typically, wires with a diameter of 50µm have a maximum frequency of about 1 Hz (Teh, 2007).

Though this research could prove very extensive, it could help allow humans to both understand better the world in which we live and to create microrobots capable of completing tasks currently impossible.

References

Çengel, et all. Fluid Mechanics: Fundamentals and Applications. New York: McGraw Hill, 2006.

Beer, Ferdinand P., et all. Mechanics of Materials. 4th ed. New York: McGraw Hill, 2003.

Mueller, T. J., Fixed and Flapping Wing Aerodynamics for Micro Vehicle Applications. Reston, Virginia: American Institute of Aeronautics and Astronautics, Inc. 2001.

Chris Kjelgaard, Aviation. World's Smallest Camera Plane Shows Off in Public. <http://www.aviation.com/> July 2008.

Bai, Ping, et all. A new bionic MAV's flapping motion based on fruit fly hovering at low Reynolds number. Beijing: China Academy of Aerospace Aerodynamics. September 2007.

Tamai, Masatoshi, et all. Aerodynamic Performance of a Corrugated Dragonfly Airfoil Compared with Smooth Airfoils at Low Reynolds Numbers. Beijing: Chinese Academy of Sciences. January 2007.

Guo, Theresa. Design and Prototype of a Hovering Ornithopter Based on Dragonfly Flight. Cambridge: MIT. June 2007.

Liu, Teresa. Design of a Flapping Mechanism for Reproducing the Motions at the Base of a Dragonfly Wing. Cambridge: MIT. June 2007.

May, Micheal L. Dragonfly Flight: Power Requirements at High Speed and Acceleration. New Brunswick: Rutgers. February 1991.

Mols, Bennie. Flapping micro plane watches where it goes. Delft Outlook. Delft University of Technology. April, 2005.

Teh, Yee H. et all. Frequency Response Analysis of Shape Memory Alloy Actuators. Canberra Australia: Australian National University. 2007.

Worley, Darren. New MAV Ornithopter – Flapping Wings Forum. Ornithopter.org. January 2006.

Leung, Kin Y. Micro-Aerial Vehicle (MAV) Research: The Developtment of a Biplane Ornithopter. University of New South Wales. 2002.

Technology Review – Young Innovators Under 35. Robert Wood – Harvard. Building Robotic Flies. 2008

Weis-Fogh, Torkel. Quick Estimates of Flight Fitness in Hovering Animals, Including Novel Mechanisms for Lift Production. Cambridge, England. January 1973.

Olson, D. H., et all. Wind Tunnel Testing and Design of Fixed and Flapping Wing Micro Air Vehicles. Tucson: University of Arizona.

Beer, Ferdinand et all. Mechanics of Materials, 4th ed. New York: Mc Graw Hill. 2006.

Hibbeler, R. C. Engineering Mechanics: Statics & Dynamics, 11th ed. Upper Saddle River, NJ: Pearson Prentice Hall. 2007.

Appendix A
Characteristics and analysis of the WowWee model

Appendix B
Characteristics and analysis of the cut down WowWee model

Appendix C
Scaling and design of the scaled prototype

Appendix D
The analytical model

Appendix E
Characteristics and analysis of the scaled prototype